Photon Netw Commun
DOI 10.1007/s11107-016-0652-1

ORIGINAL PAPER

# Energy efficient adaptive optical CDMA random access protocol based on particle swarm optimization

**Fábio Renan Durand**[1] · **Taufik Abrão**[2]

Received: 18 May 2015 / Accepted: 7 July 2016


**Abstract** In this paper, an energy efficient adaptive optical code division multiple access (OCDMA) random access protocol based on particle swarm optimization (PSO) is described. This protocol is based on the S-ALOHA with power and rate allocation based on PSO. This scheme evaluates jointly optimal power and rate allocation PSO based under the random access protocol as a new and simplified scheme for high performance, high energy efficiency suitable for OCDMA systems. The aim is to maximize the aggregate throughput, subject to predetermined quality of service restrictions and energy efficiency constraint in terms of the signal-to-noise-plus interference ratio of each user class. Numerical results are discussed taking into account realistic network operation scenario.

**Keywords** Optical networks · Random access protocol · Energy efficiency · Multiple access interference · OCDMA · Heuristic optimization · Particle swarm optimization · PSO algorithm

## 1 Introduction

The rapid increase in access networks traffic has motivated the development of energy efficient and cost-effectiveness schemes to obtain all-optical multi-access networking [1–3]. Passive optical networks (PON) are expected to meet a wide range of services with distinct and variable demands on bit rate, quality of service (QoS) and frequency use [1]. Consequently, it is necessary to forecast flexible networks that simultaneously support legacy and new services. These networks must provide maximum reuse of previous optical infrastructure, flexible bandwidth upgradeability and control, apart from capability to provide higher capacity and split ratio than existing access networks. In this scenario, it is necessary to increase energy saving in access networks, since low energy efficiency is beholden in the access equipment [4]. The future trends of access technologies involve wavelength division multiplexing (WDM), orthogonal frequency division multiple access (OFDMA) and optical code division multiple access (OCDMA) [1]. These technologies can provoke new disruptive solutions, and it can potentially meet the above requirements. OCDMA technology will be analyzed in this work; on the other hand, researches of PON-OFDM and PON-WDM are available in [5,6], respectively. OCDMA-based technology has attracted vast interests due to its various characteristics such as asynchronous operation, high network flexibility, protocol transparency, simplified network control, QoS in the physical layer and potentially enhanced security [7,8]. In the OCDMA networks the studies are focused on the physical layer [7,8], but there are a lot of challenges on the link and network layer. Several studies have shown the need to consider the random access protocol or medium access control (MAC) that avoid the throughput degradation, protocols that provide variable transmission rate, as well as provide different QoS classes for different users [9–12]. The slotted ALOHA (or S-ALOHA) is a better protocol when the user's activity and the offered traffic are high, whereas the other one like round-robin receiver/transmitter ($R^3T$) is better for smaller values of user activity and moderate traffic [13]. However, the $R^3T$ higher performance is reached at the damage of higher delay and system complexity. In the literature is inexpressive the number of works that has assumed the non-

✉ Fábio Renan Durand
fabiodurand@utfpr.edu.br

[1] Department of Electrical Engineering, Technological University of Paraná - UTFPR, Av. Albert Carazzai, Cornélio Procópio, Brazil

[2] Londrina State University, Londrina, Brazil

Published online: 01 August 2016

ideal equal received power from all the nodes to design the random access protocols and MAC [14], despite the throughput of the network being strongly affected by the near–far problem [14]. The resource allocation strategies could be utilized to regulate the transmitted power with objective to avoid the near–far problem; however, the resource allocation strategies can provide the variation of bit rate and the number of active users. These kinds of strategy are applied in order to maximize the aggregate throughput of the optical networks; specially, the deployment of resource allocation heuristics-based optimization algorithms, such as genetic algorithm (GA), particle swarm optimization (PSO) and ant colony optimization (ACO) are very promising [15,16]. However, energy efficiency aspects have not been largely investigated in the context of resource allocation. This issue has become very important since energy consumption is dominated by the PONs due to the large amount of passive network elements [4].

The contribution of this work consists in the performance analysis of energy efficient adaptive optical CDMA random access protocol. This protocol is based on the S-ALOHA with power and rate allocation based on heuristic optimization approach. The objective is to propose and evaluate the performance of a hybrid optimization procedure capable to evaluate jointly the optimal power and rate allocation deploying PSO-based algorithm under the random access protocol as an optimization scheme of reaching high performance with high energy efficiency suitable to OCDMA systems. We are interested to maximize the aggregate throughput, subject to predetermined QoS restrictions and energy efficiency constraint in terms of the signal-to-noise-plus interference ratio (SNIR) of each optical user class. The PSO is a meta-heuristic based on the movement of a population (swarm) of individuals (particles) randomly distributed in the search space, each one with its own position and velocity. The PSO-based optimization method is attractive due to its performance–complexity trade-off and fairness features regarding the optimization methods that deploy matrix inversion, purely numerical procedures and other heuristic approaches [11,15]. The PSO performance for resource allocation problem can guarantee fast convergence and fairness under a few of iterations regarding the other heuristics as GA based [15]. The S-ALOHA adaptive random access protocol supports a broad variety of multimedia services, such as data, voice, image and video, and it is able to arrange simultaneously all kinds of subscribers with very different bit rates and QoS constraints. For this purpose, the OCDMA is able to take advantage of multi-length 2-D wavelength-hopping/time-spreading code namely multiple-length extended wavelength-hopping prime code (MLEWHPC) [17]. These codes can be applied to PON-OCDMA networks to support the prioritization of services of different media, which is very important for a network to guarantee the QoS for those media (namely, video) that require high bit rate and real-time support. As distinct from conventional single-length codes, the performance of MLE-WHPCs becomes better as the code length decreases; i.e., the high-bit-rate media, such as video, will have better performance than lower-bit-rate media, for instance voice. It was showed that higher rate media have better performance than lower rate media because the long matrices used by lower rate media suffer from stronger interference created by multiple copies of the short matrices used by high-rate media [17].

The paper is organized in the following manner. The related work is discussed in Sect. 2. In Sect. 3, the mean features of the PON-OCDMA architecture are revisited, while Sect. 4 discusses how the proposed optimization scheme with adaptive random access protocol (ALOHA) and power and rate allocation can be applied to PON-OCDMA networks. Section 5 describes the adopted performance evaluation metric and methodology in order to improve the throughput and capacity of the optical network. Numerical results are analyzed in Sect. 6. Finally, the main conclusions are offered in Sect. 7.

## 2 Related work

In this section, a non-exhaustive literature review regarding random and MAC access protocols, power and rate allocation are discussed in the context of our work. In [18], two different protocols with and without pre-transmission coordination have been proposed, while the round-robin receiver/transmitter $R^3T$ protocol was proposed in [19]; indeed, the effect of several design parameters on the system performance measures has been investigated numerically for both. The results from [18,19] showed that a higher performance is achieved by the $R^3T$. In [13], the $R^3T$ and S-ALOHA protocol were compared and it was observed that both protocols could be competitive in terms of system throughput for moderate offered traffic. However, the $R^3T$ protocol suffers a higher delay mainly because of the presence of additional modes (acknowledgement mode and requesting mode). In addition, the $R^3T$ higher performance is reached at the higher system complexity. In [20], a MAC protocol with variable length data traffic was proposed. This protocol exhibits a sliding window with variable size. In [21], a protocol based on selective retransmission technique was proposed and it was compared with the $R^3T$ protocol. The results from [20,21] showed that a higher performance of $R^3T$ is achieved by the proposed protocol at the expense of system complexity. In [22], the effect of shot and thermal noise and chromatic dispersion on the performance of the $R^3T$ protocol was examined. It was found out that there are optimum values for the transmitted power to compensate for this degradation. In [23] was proposed a new hybrid sys-

tem that combines a variable transmission rate optical with the S-ALOHA protocol as scheme of achieving multirate in OCDMA networks. A variable transmission rate is achieved by overlapping among bits in a single time slot. The proposed scheme in [23] was optimized in [10] as a joint transmission power and overlapping coefficient (transmission rate) allocation strategy via the solution of a constrained convex quadratic optimization problem. It first obtains the transmission power allocations, which are determined as a function of the QoS and the transmission rate of each class. It then maximizes the aggregate throughput with respect to the transmission rate vector. In this case, the throughput function is a concave function, and therefore, the Kuhn–Tucker (KT) condition is sufficient to analytically determinate an optimal operation point. It was used the Lagrange multiplier method in order to obtain the maximum of the throughput function. The optimization processing approach of [10,23] is not attractive due to its performance–complexity trade-off. In [24], a random access protocol based on the function of automatic retransmission request (ARQ) was proposed and evaluated utilizing a new mathematical model, i.e., processor-sharing system. It is shown that the performance of the proposed protocol outperforms that of protocols proposed in [19,21], at the expense of system complexity. In this case, the sink should have the ability to detect packet errors, which can be implemented by cyclic redundancy correction (CRC). In [12], a MAC protocol that uses multilevel optical power transmission and adaptive delay adjustment to provide different QoS metrics for different users. The adaptive delay adjustment is based on the channel state observation and estimation. It has been showed that the delay adjustment procedure is able to reduce or even avoid line interference while improve overall network throughput. However, it assumed perfect channel state estimation, and there is no delay between state estimation and transmission scheduling. In [11], a fair resource allocation scheme to solve the power and rate allocation for multiclass time-slotted was proposed. However, the matrix inversion was used to solve the power allocation problem in a closed form. The matrix inversion approach is not attractive due to its performance–complexity trade-off. In [25], slotted ALOHA random access packet switching with generalized optical orthogonal code (GOOC) and M-ary overlapping pulse position modulation (OPPM) has been analyzed. The GOOCs provide significantly better steady-state and dynamic network conditions compared to the conventional on–off keying (OOK) scheme. However, in [16], the PSO algorithm was utilized to solve the problem of transmitted power allocation in order to maximize the energy efficiency of WDM/OCDM networks. Also, the main aspects and technological issues related to the power control scheme utilized in solving the near–far problem and to establish the QoS at the physical layer have been discussed [16].

In the papers mentioned in this section, it was observed that the S-ALOHA is a better protocol when the user's activity and the offered traffic are high compared with the schemes proposed in [18–21]; moreover, the S-ALOHA was previously utilized in the schemes proposed in [10,23–25]. On the other hand, some studies have presented many simplifications in the network models, such as [12], or have deployed certain approaches with high computational complexity [11]. Finally, the resource allocation strategies based on PSO could be utilized to regulate the transmitted power with objective to avoid the near–far problem and provide the variation of bit rate and the number of active users [16]. Such related issues have demonstrated the necessity to explore new schemes for access protocols integrated with power and rate allocation, aiming to maximize the aggregated throughput, subject to predetermined QoS restrictions and energy efficiency (EE) constraint.

## 3 Network architecture

In this section is presented an optical network architecture utilized in this work and the details about the OCDMA codes adopted. More information about these issues could be obtained in [1,7,8].

### 3.1 PON-OCDMA architecture

The PON-OCDMA architecture considered is formed by $K$ nodes interconnected by passive star coupler, in a broadcast-and-select pattern as showed in Fig. 1. This is a traditional model of OCDMA network architecture utilized in PON applications that could be adapted for other PON configurations [9–14,17–28]. In this network, each node has a transceiver with encoders and decoders at the transmitter and receiver. Without loss of generality, we denominated the nodes in one side of the network as transmitters ($\mathrm{Tx}_i$) and the nodes in the other side as receivers ($\mathrm{Rx}_j$). All network equipment such as code-processing devices (encoders and decoders at the transmitter and receiver) and star coupler could be made using robust, lightweight, and low-cost technology platforms with commercial-off-the-shelf technologies [26]. The transmitting and receiving nodes establish virtual paths (VP) based on the code according the OCDMA technology [7,8]. The link length of each VP is given by $d_{ij} = d_i^{\mathrm{tx}} + d_j^{\mathrm{rx}}$, where $d_i^{\mathrm{tx}}$ is the link length from the transmitting node to the star coupler and $d_j^{\mathrm{rx}}$ is the link length from the receiving node to the star coupler. The star coupler attenuation is given by $a_{\mathrm{Star}} = 10\log_{10} K - \left(\log_2 K\right) 10\log_{10}\delta$, where $\delta$ is the excess loss relation. The use of optical amplification in combination with PON-OCDMA can extend the optical link from the conventional 20 to 60–100 km [1,6].

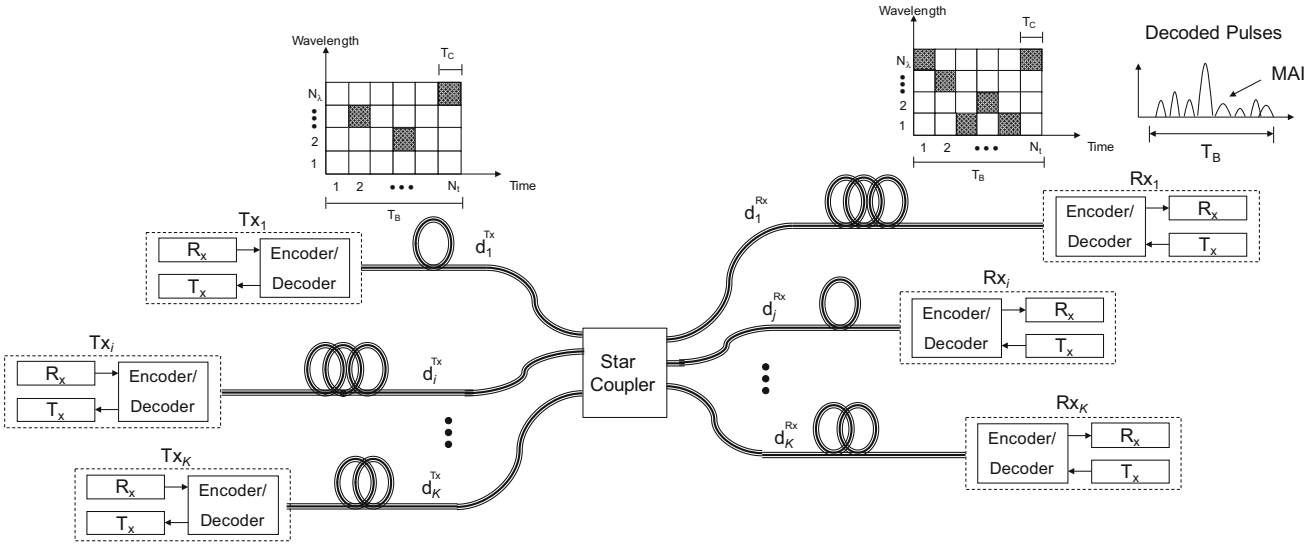


**Fig. 1** Passive optical CDMA architecture

### 3.2 OCDMA codes

The 2-D codes are defined by $N_\lambda \times N_T$ matrices, where $N_\lambda$ is the number of rows equal to the number of available wavelengths and $N_T$ is the number of columns equal to the code length [8]. Herein, the code length is determined by the bit period $T_B$ which is subdivided into small units namely chips, each of duration $T_c = T_B/N_T$. The MLEWHPC code can be derived by extending wavelength-hopping prime codes with single length. The MLEWHPCs present identical autocorrelation peaks and the cross-correlation of at most one [17]. An ($N_\lambda \times N_T$, $w$, $A$, $B$, $D$) MLEWHPC code, namely $C$, is a collection of binary {0,1} code matrices with a set of code lengths $N_T = \{n_0, n_1, \ldots, n_i, \ldots, n_{k-1}\}$, the number of available wavelengths $N_\lambda$, a code weight $w$, a set of autocorrelation constraints $A = \{\lambda_a^{(0)}, \lambda_a^{(1)}, \ldots, \lambda_a^{(i)}, \ldots, \lambda_a^{(k-1)}\}$, a set of cross-correlation constraints $B = \{\lambda_c^{(0)}, \lambda_c^{(1)}, \ldots, \lambda_c^{(i)}, \ldots, \lambda_c^{(k-1)}\}$ and a set of matrix–cardinality distributions $D = \{d_0, d_1, \ldots, d_i, \ldots, d_{k-1}\}$, where $k$ denotes the number of different code lengths in $C$. Denoting $\phi_i$ as the numbers of codes with the length $n_i$ for $i \in [1, k]$, the code with the number of available wavelengths $N_\lambda = wp'$, where $p'$ is prime number, and a set of integers $\{t_1, t_2, \ldots, t_{k-1}\}$ with $\phi_1 = (w^2 + p')(p_1 - t_1)$ code matrices of length $p_1$, $\phi_2 = (w^2 + p')(t_1 - t_2)p_2$ code matrices of length $p_1 p_2$, $\phi_3 = (w^2 + p')(t_2 - t_3)p_2 p_3$ code matrices of length $p_1 p_2 p_3$, hence $\phi_{k-1} = (w^2 + p')(t_{k-2} - t_{k-1})p_2 p_3 \ldots p_{k-1}$ is the code matrices of length $p_1 p_2 \ldots p_{k-1}$, and $\phi_k = (w^2 + p')t_{k-1} p_2 p_3 \ldots p_k$ is the code matrices of length $p_1 p_2 \ldots p_k$.

In order to avoid the need for sources that can rapidly wavelength hop, multiwavelength sources have been considered [8,17]. Therefore, the pulses can be generated from different broadband sources, such as light-emitting diodes, amplified spontaneous emission noise from erbium-doped fibre amplifier (EDFA), gain switched Fabry–Pérot lasers and super continuum generation. On the other hand, an array of mode-locked lasers, which is limited in scalability due to the higher complexity in controlling a large number of lasers could be utilized to generate the pulses [26]. The multiple access interference (MAI) between the codes is computed by the cross-correlation functions, which are obtained by correlating the node's address matrix and the received interfering matrices with shorter, identical and longer lengths [17]. Furthermore, the tunable OCDMA 2-D encoder creates a combination of two patterns: a wavelength-hopping pattern and a time-spreading pattern. The encoders–decoders are able to perform these two patterns independently, such as the array waveguide gratings (AWGs) or thin-film filters (TFFs), or simultaneously as fibre Bragg gratings (FBGs), holographic Bragg reflectors (HBRs), or chirped Moire gratings (CMGs) [26]. For instance, considering the MLEWHPC codes the encoders–decoders based on AWGs or FBG have been utilized [17]. The AWG encoder/decoder presents a uniform loss of 6 dB independently of the number of wavelengths (N) [26]. In this context, the AWG encoder/decoder is utilized in this work.

## 4 Proposed power–rate allocation scheme for OCDMA S-ALOHA

This section explains how the proposed random access control and resource allocation scheme operates over the OCDMA system, as depicted in Fig. 2. The proposed adap-

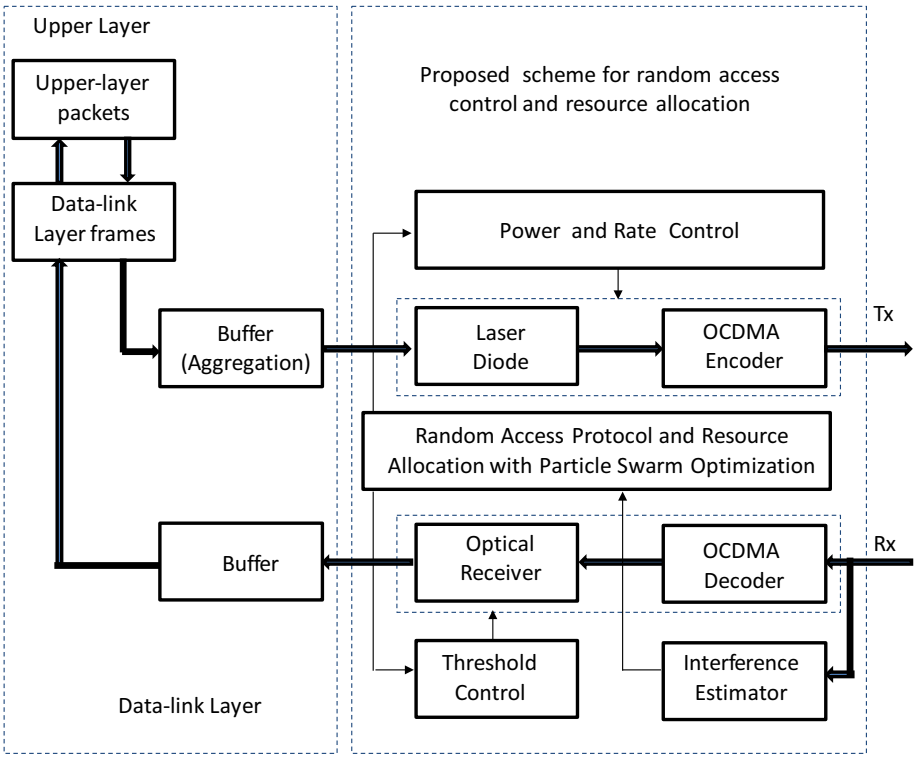


**Fig. 2** Proposed scheme based on heuristic optimization approach

tive optical CDMA random access protocol S-ALOHA scheme with PSO-based power and rate allocation is illustrated in Fig. 2. The proposed scheme is allocated in the transceiver (Tx/Rx) of Fig. 1. The overall OCDMA system consists of an optical transmitter, an optical receiver, a power and rate control mechanism, an interference estimator module, a threshold control, a random access control and resource allocation module. The deployed components and devices are detailed in [4,7–9,16,26]. Herein, the focus is on the integration of random access scheme and the PSO-based resource allocation optimization.

In Fig. 2, the receiver signal is monitoring to verify the channel conditions aiming to obtain the interference estimation in each node. The interference estimation feeds the PSO-based resource allocation optimization to jointly evaluate the optimal power and rate allocation problem. In addition, the level of interference will determine the threshold level. The procedure to determine the threshold value is not discussed in this work considering the consistent works addressing this topic [8,12]. Therefore, the proposed scheme depends on the local parameters obtained by the estimation of the interference level via the signal-to-noise-plus-interference ratio (SNIR), as well as monitoring the channel conditions. These measurements are taken normally in each ONU; therefore, there is no increasing on the complexity of the equipment. The proposed system is described as following. Primarily, the system is unoccupied and nodes generate new packets with probability $P_o$ and with well-established QoS requirements, including maximum BER, maximum optical power level and minimum bit rate. Our proposed resource allocation scheme jointly evaluated the optimal power and bit-rate allocation problem subject to predetermined QoS and energy efficiency (minimum or target) constraints in terms of minimum achievable SNIR per user class. Most of the transmitted packets will be received correctly with a probability $P_c$, while a few will be received in error with a probability $P_e = 1 - P_c$. The packet error probability occurs due to collision, channel conditions and multiple access interference (MAI).

The proposed system model with aggregate resource allocation mechanism and S-ALOHA random access with the objective to describe the node packet errors is illustrated in Fig. 3. The node whose packets are incorrectly received is backlogged, and it retransmits the packets after a random delay with a probability $P_r$. Each backlogged node stores the blocked packets, and it cannot generate new packets until all the backlogged packets are correctly retransmitted. As illustrated in Fig. 3, for the retransmission of the backlogged packet, the resource allocation scheme will jointly evaluate the optimal power and rate allocation considering the conditions of the optical channel subject to predetermined QoS and energy efficiency constraints. When a backlogged packet is retransmitted, it leaves out the buffer to be optically modulated and transmitted over the optical channel.

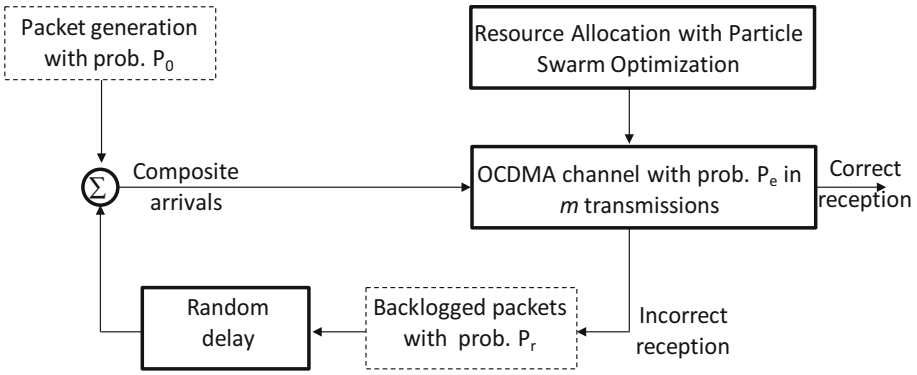


**Fig. 3** Proposed system model with resource allocation and S-ALOHA random access

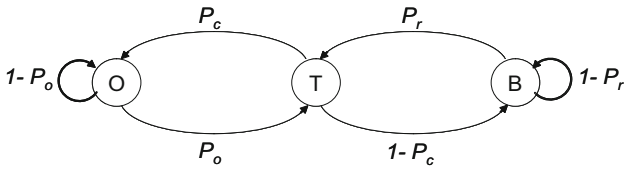


**Fig. 4** Traffic model based on general Markov chain

## 5 Optimization problem formulation and performance evaluation

In this section, the methodology for performance evaluation of the proposed scheme is discussed. Firstly, the traffic model of random access protocol S-ALOHA is presented and the effect of the PSO-based resource allocation optimization is analyzed. The optimal resource (rate and power/energy) allocation directly depends on the channel conditions quantified by the packet error rate (PER). Finally, a description for our resource allocation algorithm based on heuristic optimization is provided.

In the S-ALOHA, the traffic is apportionment according to the user's activity and the adopted traffic model is based on the general Markov chain, as illustrated in Fig. 4. In this representation, each node can be in one of the three modes at a time: origination mode (O), transmission mode (T) or backlog mode (B) [23]. The user in the origination mode generates and transmits a new packet at the beginning of the next time slot with a probability $P_{\mathrm{o}}$. The user enters the backlog mode when an attempt to transmit a new packet fails. This fails occur with probability $P_{\mathrm{e}} = 1 - P_{\mathrm{c}}$, where $P_{\mathrm{c}}$ is related to the bit error probability ($P_{\mathrm{b}}$) by $P_{\mathrm{c}}(i) = [1 - P_{\mathrm{b}}(i)]^{\vartheta}$, with $\vartheta$ the packet length in bits. When the Gaussian approximation is adopted the $P_{\mathrm{b}}$ is given by $P_{\mathrm{b}}(i) = 1/2\ \mathrm{erfc}(\sqrt{\gamma_i/2})$, where $\mathrm{erfc}(\cdot)$ is the complementary error function and $\gamma_i$ is the SNIR.

The PSO is used to evaluate jointly optimal power and rate allocation subject to predetermined QoS restrictions in terms of the SNIR of each user class. The packet error probability occurs due to collision, MAI or physical imperfections of the channel. However, the packet error occurs if the QoS target cannot be reached with the total amount of available resource versus the number of optimal links to be served. The node whose packets are incorrectly received is backlogged, and it retransmits the packets after a random delay with a probability $P_{\mathrm{r}}$. To elaborate further, the retransmissions of a backlogged packet occur in any given time slot with probability $P_{\mathrm{r}}$. In the backlogged mode, the blocked terminal cannot generate new packets until the backlogged packet is received correctly. For $P_{\mathrm{r}} = P_{\mathrm{o}} = p$, the arrival distribution can be approximated by either a binomial distribution if the number of users in the system is finite or by a Poisson distribution if this number is very high. Let the conditional packet success probability be $P_{\mathrm{c}}(i)$, where $i$ packets transmit in the same time slot, the conditional mean of the number of successful packets $S$ can be expressed by $E\{S\} = P_{\mathrm{c}}(i) \cdot i$. Hence, the steady-state throughput $\beta$ is the expected number of successful packets per slot given by [23]

$$\beta = \sum_{i=1}^{\infty} i \cdot f_I(i) \cdot P_{\mathrm{c}}(i) \tag{1}$$

where $f_I(i)$ is the probability mass function for the arrival process $I$. The arrival distribution $I$ could be approximated by a binomial distribution, the steady-state throughput is written as:

$$\beta = \sum_{i=1}^{K} i \cdot \binom{K}{i} \left(\frac{\bar{G}}{K}\right)^{i} \left(1 - \frac{\bar{G}}{K}\right)^{K-i} P_{\mathrm{c}}(i) \tag{2}$$

where $\bar{G}$ is the average offered traffic rate. The average offered traffic is composed of the newly generated successfully transmitted packets and successfully retransmitted packets, and it is computed as [14]

$$\bar{G} = (K - \bar{n})\, P_{\mathrm{o}} + \bar{n} P_{\mathrm{r}} \tag{3}$$

where $\bar{n}$ is the expected channel backlog. The average packet delay is defined by Little's theorem as the average number of backlogged users over the system throughput as [23]

$$D = \frac{\bar{n}}{\beta} + 1 \tag{4}$$

In multirate multiple access optical communications networks, the BER is often used as a QoS measure and since the BER is inversely proportional to the SNIR, we are able to use the SNIR parameter as the QoS measurement. Hence, associating the SNIR to the carrier-to-interference ratio (CIR) of the $i$th node in an OCDMA network at time slot $n$ results:

$$\gamma_i = \frac{r_c}{r_i} \times \Gamma_i \tag{5}$$

where $r_i$ is the achievable information rate (bits/s) for the $i$th node, $r_c$ is the available system chip rate (bandwidth), and $\Gamma_i$ is the CIR at the input of $i$th node, given by [28],

$$\Gamma_i = \frac{G_{ii}\, p_i}{\sum_{j=1, j\neq i}^{K} G_{ii}\, p_i + \sigma_i^2} \tag{6}$$

where $G_{ii}\, p_i$ is the received power at the $i$th node, $\sigma_i^2$ is the power of receiving noise, and the elements $G_{ij}$, that represent the connection gains of transmitter–receiver pairs, constitute the network attenuation matrix, given by:

$$G = \begin{bmatrix} G_{11} & \ldots & G_{1K} \\ \vdots & \ddots & \vdots \\ G_{K1} & \ldots & G_{KK} \end{bmatrix} \tag{7}$$

where $G_i\, j$, for all $i \neq j$, corresponding the attenuation factor from the interferer user's signal $j$ to the interest user's signal, $i$. Note that, the usual receiver noise power $\sigma_i^2$ in (6) includes thermal noise, shot noise and optical preamplifier noise. Note that the amplifier spontaneous emission (ASE) effect in the optical preamplifier will be one of the main limiting factor (in addition to the MAI), compared to thermal and shot noise at the receiver side [28]. Furthermore, the receiver noise power is suitably represented as $\sigma_i^2 = 2 n_{SP} h f\, (G_i - 1)\, B_0$, which take into account the two polarization mode presented in a single mode fibre, and where $n_{SP}$ is the spontaneous emission factor, typically around $2 \sim 5$, $h$ is Planck's constant, $f$ is the carrier frequency, $G_i$ is the amplifier gain and $B_0$ is the optical bandwidth. In our context, the ASE can be well represented by a random classical optical field that has the statistical properties of an additive Gaussian noise. Herein, the power spectral density of ASE is assumed to be equivalent to the power spectral density of the additive white Gaussian noise. Therefore, the Shannon channel capacity for spread spectrum systems considering the gap between theoretical bound and the effective information rate (multirate) can be defined as in [27]:

$$\mathrm{r}_i = \frac{\omega_i}{m_i} \log_2 (1 + \theta_i \gamma_i) \tag{8}$$

where $m_i = \log_2 M_i$ is the modulation order, $\theta_i$ is the inverse of the gap between the theoretical bound and the real information rate, $\omega_i$ is the user's non-spreading equivalent signal bandwidth, and $r_c$ is the available system bandwidth. Usually, $\theta_i$ can be approximated by [29]:

$$\theta_i = -\frac{1.5}{\log\left(5 \cdot \mathrm{BER}_i^{\max}\right)} \tag{9}$$

where $\mathrm{BER}_i^{\max}$ is the maximum tolerable bit error rate for the $i$th node' service. In order to enable the users to have minimum QoS guarantee, the minimum CIR to SNIR relation must be calculated as

$$\Gamma_{i,\min} = \frac{r_{i,\min}}{r_c} \times \gamma_i^* \tag{10}$$

where $\Gamma_{i,\min}$ and $r_{i,\min}$ are the minimum CIR and minimum information rate for the $i$th user, respectively, and $\gamma_i^*$ is the minimum (or target) SNIR needed for the network reaches the acceptable per user basis QoS associated with the maximum tolerable BER per user of each service class.

### 5.1 Optical power–rate optimization problem formulation

The optimal SNIR depends on the power and rate of each optical CDMA user/node. Hence, our SNIR optimization is based on the definition of the minimum power constraint (also called sensitivity level), assuring that the optical signal can be suitably detected by all-optical devices, while the QoS requirements are hold. As a consequence, the power control in optical CDMA networks can be seen as an optimization problem. Thus, denoting $\Gamma_i$ at the required decoder input, in order to get a certain maximum tolerable bit error rate at the $i$th optical node ($\mathrm{BER}_i^{\max}$), and defining the $K$-dimensional column vector of the transmitted optical power $\mathbf{p} = [p_1, p_2, \ldots, p_K]^{\mathrm{T}}$, the optical power control problem consists in finding the optical power vector $\mathbf{p}$ that minimizes the cost function $J_1(\mathbf{p})$ this optimization problem can be formally described as [28]:

$$\begin{aligned} &\min_{p\in \boldsymbol{K}^+} J_1(\mathbf{p}) = \min_{p\in \boldsymbol{K}^+} 1^{\mathrm{T}}\mathbf{p} = \min_{p\in \boldsymbol{K}^+} \sum_{i=1}^{K} p_i \\ &\text{subject to}: \quad \Gamma_i = \frac{G_{ii}\, p_i}{\sum_{j=1, j\neq i}^{K} G_{ii}\, p_i + \sigma_i^2} > \Gamma_i^* \\ &\qquad\qquad p_{\mathrm{mim}} \leq p_{\mathrm{i}} \leq p_{\max} \quad \forall i = 1, \ldots, K, \end{aligned} \tag{11}$$

where $\mathbf{1}^{\mathrm{T}} = [1, \ldots, 1]$ is a one vector and $\Gamma_i^*$ is the minimum CIR to achieve a desired QoS; $P_{\min}$ and $P_{\max}$ are the minimum and maximum value considered as allowable transmitted power, respectively. Using matrix notations, (11) can be written as $[\mathbf{I} - \boldsymbol{\Gamma}^* \mathbf{H}] \geq \mathbf{u}$, where $\mathbf{I}$ is the identity matrix, $\mathbf{H}$

is the normalized interference matrix, which elements evaluated by $\mathrm{H}_{ij} = \mathrm{G}_{ji}/\mathrm{G}_{ii}$ for $i \neq j$ and zero for another case, thus $\mathrm{u}_i = \Gamma^* \sigma_i^2/\mathrm{G}_{ii}$, where there is a scaled version of the noise power. Substituting inequality by equality, the optimized power vector solution can be analytically obtained through the matrix inversion $\mathbf{p}^* = [\mathbf{I} - \mathbf{\Gamma}^* \mathrm{H}]^{-1}\mathbf{u}$. However, the matrix inversion is not attractive procedure due to its performance–complexity trade-off [11,15]. The optimization method to obtaining the optical power vector $\mathbf{p}$ based on PSO is a expeditious method in order to solve resource allocation problems due to its performance–complexity trade-off and fairness features regarding the optimization procedure based on matrix inversion [14–16].

An alternative formulation to the power allocation optimization of (11) is discussed in [16] and adopted herein with some adaptation in order to jointly include rate and power allocation:

$$\max_{p \in \boldsymbol{K}^+} J_2(\mathbf{p}) = \max_{p \in \boldsymbol{K}^+} \frac{1}{K} \sum_{k=1}^{K} \mathcal{F}_k^{\mathrm{th}} \left(1 - \frac{p_k}{P_{\max}}\right)$$
$$\text{subject to}: \gamma_k \geq \gamma_k^*, \quad 0 < p_k^l \leq P_{\max}, \quad R^l = R_{\min}^l \forall k \in K_l,$$
$$\text{and } \forall l = 1, 2, \ldots, L \tag{12}$$

where $L$ is the number of different group of information rates allowing in the system and $k_l$ is the number of user in the $l$th rate group with minimum rate given by $R_{\min}^l$. Finally, the threshold function in (12) is defined as:

$$\mathcal{F}_k^{\mathrm{th}} = \begin{cases} 1, & \gamma_k \geq \gamma^* \\ 0, & \text{otherwise} \end{cases} \tag{13}$$

where $\gamma_k$ is the SNIR for the $k$th user. Note that, the term $1 - \frac{p_k}{p_{\max}}$ gives credit to those solutions with minimum power and punishes others using high power levels.

### 5.2 PSO principle

In the heuristic PSO procedure, each particle keeps track of its coordinates in the space of interest, which are associated with the best solution (fitness) it has achieved so far. Another best value tracked by the global version of the particle swarm optimizer is the overall best value, and its location, obtained so far by any particle in the population. At each time iteration step, the PSO concept consists of velocity changes in each particle toward local and global locations. Acceleration is weighted by a random term, with separate random numbers being generated for acceleration toward local and global locations. Let $b_p$ and $v_p$ denote a particle coordinates (position) and its corresponding flight speed (velocity) in a search space, respectively. In the PSO strategy, each power vector candidate $\mathbf{b}_p[t]$, with dimension $k \times 1$, is used for the velocity vector calculation of the next iteration [15,16]:

$$\mathbf{v}_p[t+1] = \omega[t]\,\mathbf{v}_p[t] + C_1 \mathbf{U}_{p_1}[t] \left(\mathbf{b}_p^{\mathrm{best}}[t] - \mathbf{b}_p[t]\right) + C_2 \mathbf{U}_{p_2}[t] \left(\mathbf{b}_{\mathrm{g}}^{\mathrm{best}}[t] - \mathbf{b}_p[t]\right) \tag{14}$$

where $\omega[t]$ is the inertia weight of the previous velocity in the current speed calculation, the velocity vector has $K$ dimension $\mathbf{v}_p[t] = [v_{p_1}^t v_{p_2}^t \ldots v_{p_k}^t]^{\mathrm{T}}$; the diagonal matrices $\mathbf{U}_{p_1}[t]$ and $\mathbf{U}_{p_2}[t]$ with dimension $K$ have their elements as random variables with uniform distribution in the range $U \in [0, 1]$, generated for the $p$th particle at iteration $t = 1, 2, \ldots, \mathcal{G}$; $\mathbf{b}_{\mathrm{g}}^{\mathrm{best}}[t]$ and $\mathbf{b}_p^{\mathrm{best}}[t]$ are the best global vector position and the best local vector position found until the $t_{\mathrm{th}}$ iteration, respectively; $C_1$ and $C_2$ are acceleration coefficients regarding the best particles and the best global positions influences in the velocity updating, respectively.

In our power allocation problem, the $p_{\mathrm{th}}$ particle's position at the $t$th iteration is defined by the power candidate-vector $\mathbf{b}_p[t] = [\mathrm{b}_{p1}^{\mathrm{T}} \mathrm{b}_{p2}^t \ldots \mathrm{b}_{pk}]^{\mathrm{T}}$ . The position of each particle is updated using the new velocity vector for that particle,

$$\mathbf{b}_p[t+1] = [\mathbf{b}_p[t] + \mathbf{v}_p[t+1], \quad p = 1, \ldots, \mathcal{P} \tag{15}$$

where $\mathcal{P}$ is the population size.

### 5.3 Performance metric and optical channel estimation

The quality of solution achieved by any iterative resource allocation procedure could be measured by how close to the optimum solution is the found solution and can be quantified by the normalized mean squared error (NMSE) when equilibrium is reached. For power allocation problem, the NSE definition is given by,

$$\mathrm{NMSE}[t] = \mathbb{E}\left[\frac{||\mathbf{p}[t] - \mathbf{p}^*||^2}{||\mathbf{p}^*||^2}\right] \tag{16}$$

where $||\cdot||^2$ denotes the squared Euclidean distance to the origin and $\mathbb{E}[\cdot]$the expectation operator. In addition, another performance metric called rate of convergence is utilized. The rate of convergence can be described as the ratio of PSO solution after the $t$-th iteration divided by the PSO solution after total convergence, which in this optimization context is given by the matrix inversion solution. In this work, it is not considered the perfect optical channel state estimation and there is an uncertainty in the SNIR estimation in each iteration/updating of the proposed scheme. The SNIR estimations at each node are not perfect and some parameters the received samples depend not only on the transmitted pulse shape, filter types and bandwidths, but also on the optical channel impairments, mainly group velocity dispersion (GVD), polarization mode dispersion (PMD) and noise power spectral density (PSD) [22]. Due to the square-law nature of a

photodiode, the estimation of the required channel parameters is not straightforward. The values, obtained from these estimations, present a random error characteristic. In order to incorporate this characteristic, a random error is added to the each channel gain coefficient ($G_{ii}$) and in the calculated SNIR, at each iteration of the resource allocation optimization procedure. The estimated channel matrix ($\widehat{\mathbf{G}}$) to the true channel matrix ($\mathbf{G}$) ratio values is modeled by $(1+\varepsilon)$, where will be considered as the random variable with a uniform distribution within a range of $[\pm\delta]$; hence, the estimated channel matrix$\widehat{\mathrm{G}}$, at each iteration, is given by:

$$\widehat{\mathbf{G}} = (1+\varepsilon)\mathbf{G}, \quad \forall\, i \text{ and } \varepsilon \in [-\delta;\, \delta] \tag{17}$$

In our proposed resource allocation A-OCDMA scheme, each optical node independently adjusts its transmitter power in an attempt to maximize the number of transmitted bits with minimum consumption of energy. The energy necessary for 1 bit transmission on each optical code can be expressed as $E_i = p_i T_{\text{bit}}$, where $T_{\text{bit}} = 1/R$ is the time to transmit one bit over the network, where $R$ is the bit rate.

### 5.4 Computational complexity

This subsection discusses the computational time and computational complexity of the proposed PSO-based adaptive optical CDMA random access protocol. The computational complexity usually refers to the upper bound for the asymptotic computational complexity, which quantifies the amount of time taken by an algorithm to run as a function of their input size, number of mathematical operations, as well as the number of iterations to obtain the algorithm convergence. In the our proposed PSO-based resource allocation scheme, the computational complexity is given by $\mathcal{O}\left(K^2\right)$, where $K$ is the number of nodes in the network. This computational complexity is obtained in the same way of [30]. For comparison proposes, for the matrix inversion, the computational complexity considering the best situation is given by $\mathcal{O}\left(K^2 \cdot \log K\right)$ [31].

On the other hand, without loss of generality, the overall delay in PONs is composed by the queuing delay, packet transmission and propagation delays. Other delay components depend on the adopted PON technology [32,33]. The resource allocation algorithms, such as the utilized in the proposed scheme, could be performed in parallel way during data queuing process [32,33]. Therefore, the delay contribution of the proposed scheme presents low impact on the overall system delay. In this context, the resource allocation algorithms depend heavily on the hardware and software used; furthermore in the optical nodes (OLTs or ONUs), the proposed scheme could be performed in hardware-accelerated computation or via software. In this context, considering the simulations performed with MATLAB (version 7.1) in a computer with 32 GB of RAM and processor Intel Xeon E5-1650@ 3.5 GHz, the computational time needed for the convergence of the proposed scheme is approximately 68.8 µs. These values were obtained for one trial with the level of NMSE of $10^{-2}$. The mean packet delay presented for long-reach PONs could be in the order of 5 ms [34].

## 6 Numerical results

In all numerical results discussed in this section, typical parameter values for the optical network devices and standard fibre have been assumed and summarized in Table 1. The triple-length MLEWHPC code described in Sect. 3.2 is characterized by (9 × {11,121,1331}, 3, {1,1,1}, {1,1,1,1}, {96/4716, 264/4716, 4356/4716}) where $k = 3$, $p_1 = p_2 = p_3 = 11$, $w = p' = 3$, $t_2 = 1$ and $t_1 = 3$ [8,17].

Furthermore, assuming the $T_c = 9$ ps, we have determinate three Classes of traffic as show Table 2. The traffic in Class 3 needs the highest priority and bit rate, as high-definition video communications; Class 2 needs moderated priority and bit rate, as data traffic, and Class 1 needs lower priority and bit rate, as digitized voice. The BER distribution is given by $\text{BER}_3 < \text{BER}_2 < \text{BER}_1$ with at least one order of magnitude between two consecutive classes. The PSO performance for the (power-rate) resource allocation optimization is highly dependent on its control parameters [15]. Herein, the optimization of PSO input parameters, such as acceleration coefficients, $C_1$ and $C_2$, maximal velocity factor, $V_{\max}$, weight inertia, $\omega$ and population size, $\mathcal{P}$, regarding the power optimization for OCDM networks problem were carried out as in [16]. The best acceleration coefficient values lie on $C_1 = 1.8$ and $C_2 = 2.0$ in terms of suitable quality solution and complexity trade-off. The swarm population size has

**Table 1** Adopted OCDMA network parameter values

| Parameter | Value | Unit |
|---|---|---|
| Frequency | $f = 193.1$ | THz |
| Bandwidth | Bo = 100 | GHz |
| Gain | $G = 20$ | dB |
| $n_{SP}$ | 2 | |
| Planck's constant | $h = 6.63 \times 10^{-34}$ | J/Hz |
| Packet length | 500 | bytes |
| MLEWHPC code | Same as in [8,17] | |
| Chip period | $T_c = 9$ | ps |
| Max. laser power | $P_{\max} = 20$ | dBm |
| Min. laser power | $P_{\min} = P_{\max} - 90$ | dBm |
| Link length | Range [4; 100] | km |
| # nodes | 16 (uniformly distributed) | |
| Target SNIR | 18 and 22 | dB |

**Table 2** Traffic classes and code parameters

| | Length | $\phi$ | Bit duration | Bit rate | BER |
|---|---|---|---|---|---|
| Class 1 | 1331 | 4356 | $p_1 p_2 p_3 T_c$ | 100 Mbps | $BER_1$ |
| Class 2 | 121 | 264 | $p_2 p_3 T_c$ | 1 Gbps | $BER_2$ |
| Class 3 | 11 | 96 | $p_1 T_c$ | 10 Gbps | $BER_3$ |

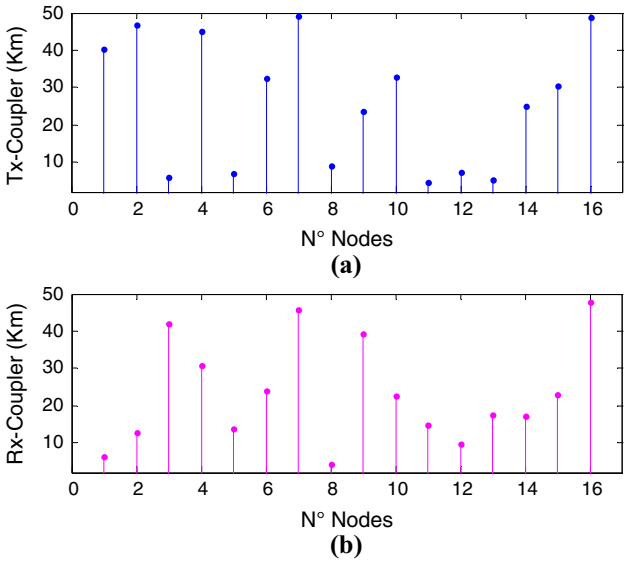


**Fig. 5** **a** Distance between Tx nodes and star coupler; **b** distance between Rx nodes and star coupler

**Table 3** Combination of nodes from different classes

| Comb | Number of nodes in each class | | |
|---|---|---|---|
| | Class 1 | Class 2 | Class 3 |
| 1 | 8 | 4 | 4 |
| 2 | 4 | 8 | 4 |
| 3 | 4 | 4 | 8 |

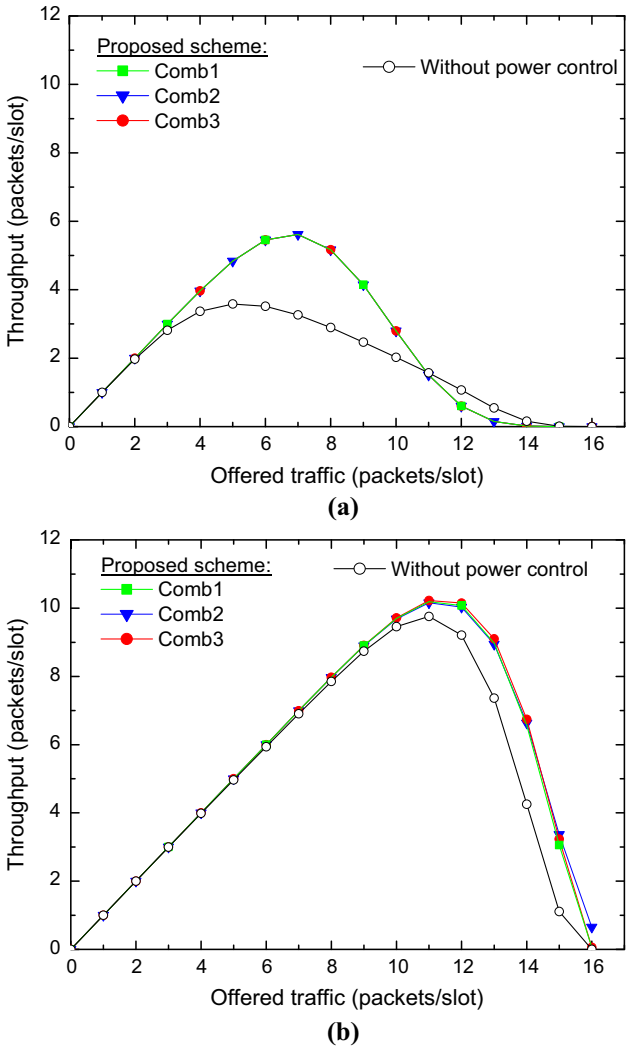


**Fig. 6** Throughput versus the offered traffic for Comb 1, 2 and 3, considering the maximum target SNIR of **a** 18 dB and **b** 22 dB

been set as $\mathcal{P} = K + 2$. Inertial weight of $\omega_{\text{initial}} \cdot V_{\max} = 0.2\,(P_{\max} - P_{\min})$ and $\omega_{\text{initial}} \cdot V_{\max} = 0.2\,(P_{\max} - P_{\min})$ with $V_{\max} = 0.2\,(P_{\max} - P_{\min})$ have been considered, where $P_{\max} = 20$ dBm and $P_{\min} = P_{\max} \times 10^{-12}$ [dBm]. Furthermore, the scenario considered in our study is represented in Fig. 5. The distances between Tx nodes and star coupler and the distances between Rx nodes and star coupler considering the 16 nodes are uniformly distributed over an area with a radius between 2 and 50 km; hence, the range of the total link length is [4; 100] km. These link lengths cover traditional PON distances and long-reach PON distances. In addition, the uniform distribution is the simplest distribution to obtain a good approximation of the system performance from other distributions [35].

For performance evaluation purpose, nodes from different classes have been grouped as illustrated in Table 3. Indeed, in Comb 1, the majority of nodes belongs to the Class 1; on the other hand, in the Comb 2 and Comb 3, the majority of nodes belongs to the Class 2 and Class 3, respectively.

In order to analyze the impact of the proposed adaptive allocation resource scheme on the throughput performance, we have depicted at Fig. 6 the throughput for the offered traffic, considering the maximum target SNIR of (a) 18 dB and (b) 20 dB. The packet length of 500 bytes for the same OCDMA network utilized in Fig. 5 was considered. Two scenarios of study have been considered, one without power control and other with the proposed scheme (with power–rate allocation). For the scenario with proposed scheme, it was considered the classes combinations of different nodes as illustrated in Table 3. For the scenario without power control, it is considered the best situation of combination of nodes and the transmitted power for each node was evaluated by a static power budget to reach the target SNIR; however for

static power budget, it were not considered deleterious MAI effects or even the number of active nodes [14].

The effects of proposed scheme on the throughput performance are depicted in Fig. 6. Indeed, one can see the proposed scheme enables the throughput maximization for the three combinations of nodes classes (Comb 1, 2 and 3). In general, when the offered traffic (packets/slot) increases, the SINR declines and the packets become more vulnerable to distortion, which reduces the likelihood of their successful transmission and reception. Thus, the probabilities of correct packets collapse, and hence, the throughput decreases.

In Fig. 6b, there is an evident difference on the throughput for the case without power control and the proposed scheme, where the peak variation of throughput reaches 35 % for the optical network operating in a more energy-efficient (EE) regime (low SNR). Besides, under the EE regime (Fig. 6a), the throughput level decreases more slowly when the traffic increases than in networks under non-EE operation (Fig. 6a). In Fig. 6a, the throughput achieved for the case without power control is very close to the throughput presented for the proposed scheme and the peak variation of throughput is approximately 5.4 %. This proximity of performance is reached at the expense of higher transmitted power for the case with no power control mechanism [28]. Furthermore, when high SNIRs are used the increment in transmitted power does not reflect in a proportional SNIR increasing, because the SNIR is near to the saturation. Aiming to analyze the behavior of the network throughput versus the packet delay in the proposed EE-based OCDMA scheme, we have depicted in Fig. 7 this effect, considering more energy efficient situation, i.e., (b) 18 dB and the maximum target SNIR of (a) 22 dB.

Indeed, one can observe that the throughput and the average packet delay increase until the throughput reaches its saturation value, characterizing an exponential behavior, where, initially the throughput is able to grow rapidly with a small delay penalty; however, near the throughput saturation limit, the delay penalty increases exponentially. This is a general trend, and the saturation value depends on the SNIR and code parameters. The proposed OCDMA with power–rate allocation strategy reduces the delay for the three combinations of nodes classes (Comb 1, 2 and 3) when compared to a system without power control mechanism. Furthermore, following the same trend observed in Fig. 6, the greater impact is observed when the energy-efficient regime and medium throughput scenarios (SNIR = 18 dB and 4–9 packet/slots in Fig. 7a) were considered; for instance, under a mean packet delay of 2 packets the variation of throughput between the proposed scheme and with no power control strategy is approximately 8 and 25 % under high SNIR regime (Fig. 7b) and EE-based regime (Fig. 7a), respectively. Figure 8 depicted the transmitted sum power of the entire network versus the number of iterations for the proposed heuristic power optimization scheme and considering the matrix inversion approach, which is plotted with the horizontal dotted lines; again, a maximum target SNIR of (a) 18 dB and (b) 22 dB have been deployed.

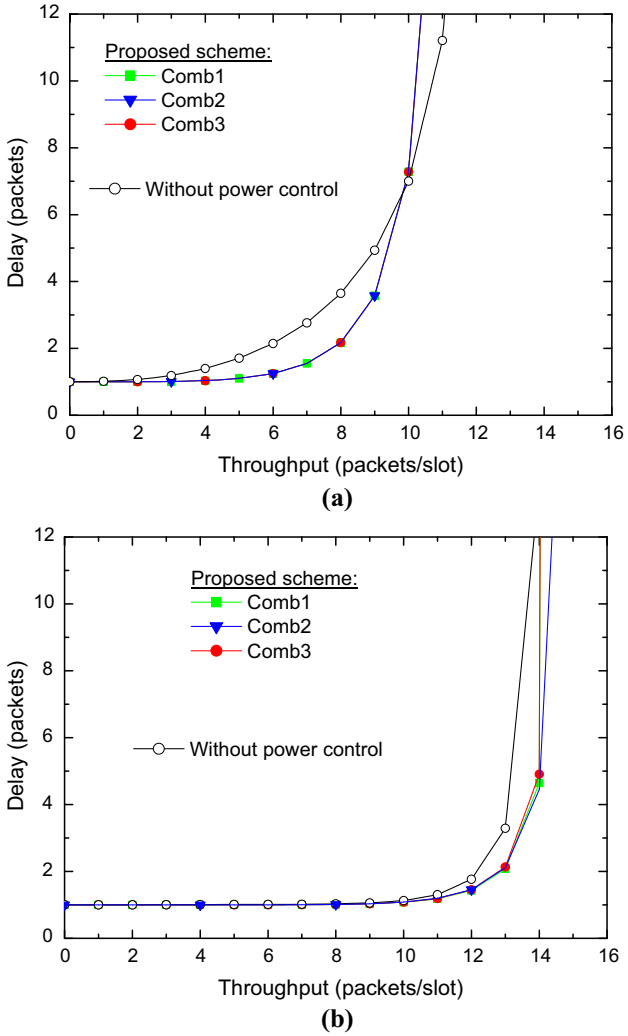


**Fig. 7** Delay versus the throughput for Comb 1, 2 and 3; maximum target SNIR: **a** 18 dB and **b** 22 dB

We can observe from Fig. 8 the convergent values for the proposed iterative heuristic optimization scheme, which alternatively could be calculated at each node by matrix inversion procedure (dot line), which becomes substantially much more intensive when the network dimension grows. On the other hand, one can observe the huge difference between the transmitted powers for each combination of nodes classes. Furthermore, the Comb 3 presents the higher level of transmitted power when compared to Comb 1 and Comb 2. This fact indicates that transmitted power increases when the number of transmitting nodes with highest priority and bit rate increases. In this context, the throughput/delay performance presented in Figs. 6 and 7 for Comb 3 (with the highest priority and bit rate) is achieved at the expense

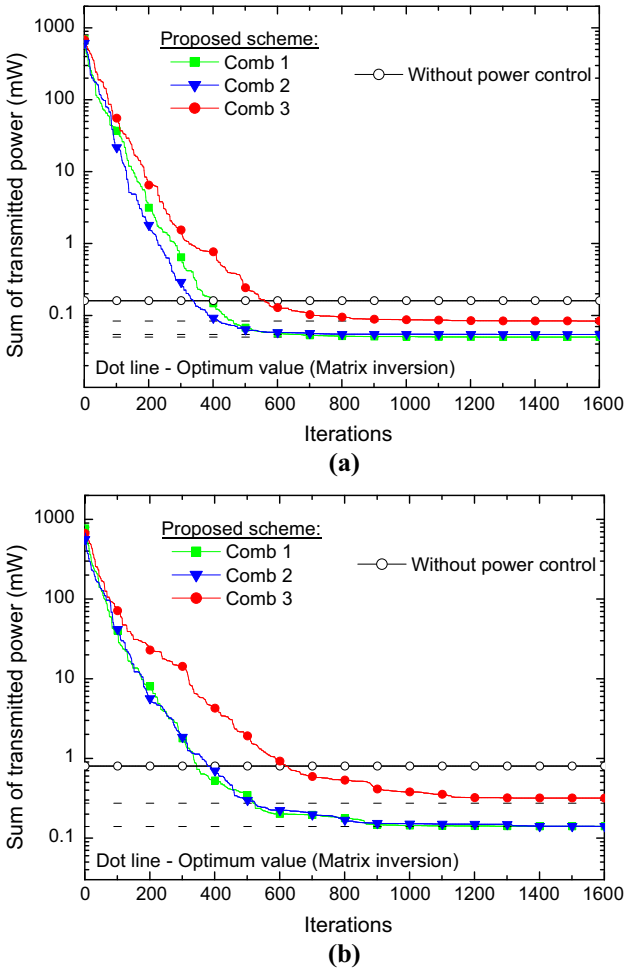


**Fig. 8** Sum of transmitted power it versus the number of iterations for Comb 1, 2 and 3; maximum target SNIR: **a** 18 dB; **b** 22 dB

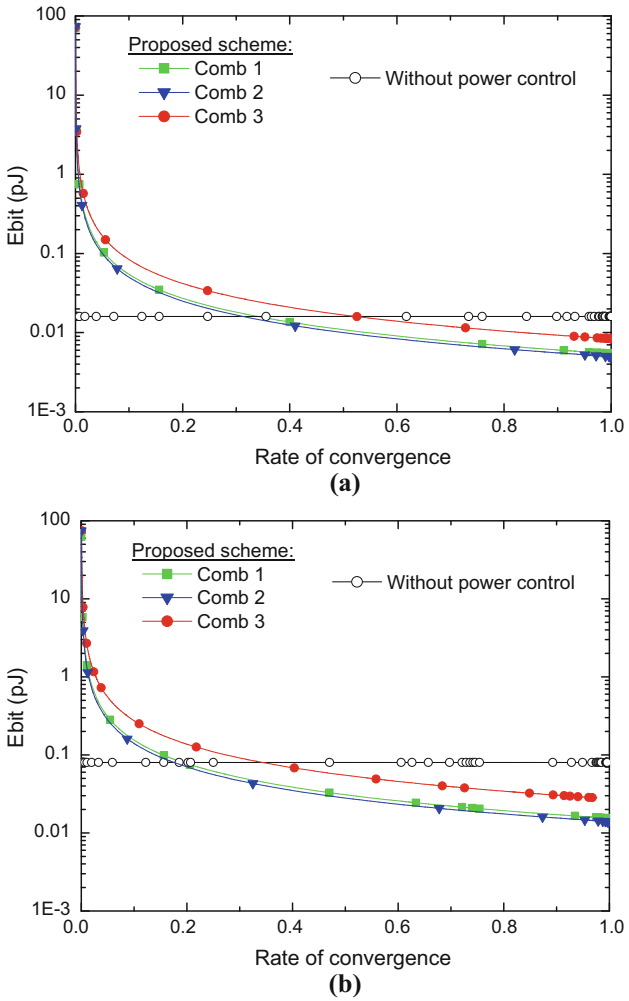


**Fig. 9** Sum of energy per bit for the network nodes versus the relative number of iterations under Comb 1, 2 and 3 classes and maximum target SNIR of **a** 18 dB; **b** 22 dB

of a higher transmitted power. Furthermore, the numerical results revealed that increasing the SNIR results in a slower convergence, since this trend produces an increasing in the multiple access interference (MAI), and, as a consequence, the heuristic PSO algorithm faces more difficult to find the global optimum.

In Fig. 8a, the sum of transmitted power for the proposed scheme is smaller than sum of transmitted power for the case without power control. The variation of sum of transmitted power for the proposed scheme after convergence and without power control is approximately 48.1, 65.6 and 69.0 % for Comb 3, Comb2 and Comb1, respectively. Herein, the throughput/delay performance presented in Figs. 6 and 7 of the system without power control is worst than the performance presented for the proposed scheme, nevertheless at the expense of higher transmitted power. Furthermore, the proposed adaptive heuristic EE-based OCDMA scheme has been demonstrated effectiveness in decreasing the transmitted power and simultaneously increasing the network performance considering the throughput and delay constraints for the case of moderated EE-based SNIR regime (18 dB).

In Fig. 8b, the same behavior of the sum of transmitted power is presented; however, the variation of the sum of transmitted power for the proposed scheme after convergence and with absence of power control mechanisms is approximately 62.5, 82.5, 82.5 % for Comb 3, Comb2 and Comb1, respectively, indicating a huge energy saving in the context of green communication policies. Besides and complementarily, the throughput/delay performance for the network without power control, depicted in Figs. 6 and 7, is achieved at the expense of much higher transmitted power. In this context, the proposed scheme is effective for the decrease in transmitted power and increase in network performance considering the throughput and delay for the case of high SNIR (22 dB).

The energy per bit ($E_{\text{bit}}$ [pJ]) spent under the EE-based OCDMA scheme is analyzed in the following. Figure 9

shows the sum energy per bit as a function of the rate of convergence of the allocated power vector under the heuristic PSO algorithm considering the same previous combinations of nodes classes (Comb 1, 2 and 3) and SNIR regimes. Hence, one can see from Fig. 9 the remarkable impact of the proposed scheme, on the network energy efficiency improvement. The deployment of PSO with 100 % of rate of convergence results in a considerable saving of energy. Indeed, with very low number of PSO iterations, typically under rate of convergence RC $<$ 0.4 and RC $<$ 0.2 for SNIR of 18 and 22 dB, respectively. The transmitted energy per bit is high, since the MAI is strongly influenced by the still remained near–far effects. As expected, the increase in nodes with highest priority and bit rate (Class 3), results in the increase in the transmitted energy per bit to reach the SNIR target.

Furthermore, one can analyze the variation of saving energy for different levels of convergence rate; for instance, the variation of saving energy regarding the rate convergence in the range RC $\in$ [0.6; 1.0] remains in approximately 50–65 % for the worst case (Comb 3), considering SNIR of 22 dB. On the other hand, the variation of saving energy regarding the rate of convergence in the range RC $\in$ [0.7; 1.0] remains approximately 25–50 % for the worst case (Comb 3) and SNIR equal to 18 dB. In summary, our numerical results have revealed the viability of the proposed scheme deployment in order to achieve higher throughput-delay trade-off performance in order to guarantee the decrease in transmitted power while increase overall network energy efficiency.

Finally, Fig. 10 depicts the NMSE for the power allocation problem, Eq. (16), as a function of the rate of convergence for the same configurations analyzed previously. The SINR estimation error was modeled in accordance with Eq. (17), with $\delta \in [0; 0.1; 0.2; 0.3]$. It can be seen from all graphs of Fig. 10 the effect of SINR error estimation under the NMSE.

The results show that even under a strong SINR error estimation of 30 % ($\delta = 0.3$), the normalized mean squared error is reduced significantly after a few number of iteration when compared to the case without power control procedure. On the other hand, the difference between the NMSE for the proposed scheme considering the case without power control depends on the SNIR. It is more significant under high SNIR regime. This behavior is illustrated in Fig. 10a, b, when the NMSE for SNIR of 22 and 18 dB are presented, respectively.

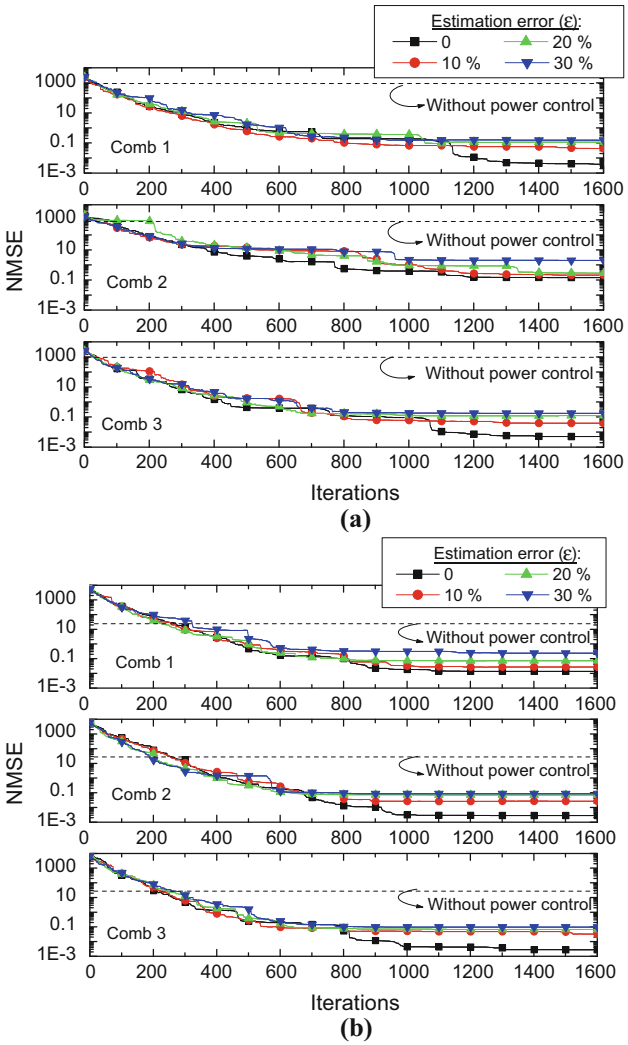


**Fig. 10** NMSE versus the number of iterations for Comb 1, 2 and 3, considering the maximum target SNIR of **a** 22 dB and **b** 18 dB

## 7 Conclusions

In this paper, an optical code division multiple access (OCDMA) random access protocol based on particle swarm optimization is investigated, aiming to increase the overall energy efficiency under different rate–user classes. This protocol is based on the S-ALOHA with power and rate allocation based on heuristic particle swarm optimization approach. The proposed iterative scheme is able to solve jointly the optimal power and rate allocation based on heuristic PSO approach under the random access protocol as a scheme to achieve high performance and high energy efficiency in optical CDMA-based communication systems. The proposed optimization scheme has been able to maximize the aggregate throughput, under predefined energy/power and quality of service (QoS) constraints, measured in terms of minimum signal-to-noise-plus interference ratio (SNIR) level of each user rate class. The application of the proposed resource allocation scheme in OCDMA systems is capable of maximizing the network performance regarding the throughput and mean packet delay in order to guarantee high energy efficiency levels while decreasing the transmitted power.

## References


[1] Wong, E.: Next-generation broadband access networks and technologies. J. Lightwave Technol. **30**(4), 597–608 (2012)

[2] Valcarenghi, L., et al.: Energy efficiency in passive optical networks: where, when, and how? IEEE Netw. **26**, 61–68 (2012)

[3] Mukai, H., Tano, F., Nakagawa, J.: Energy efficient 10G-EPON system. In: Proceedings of OFC/NFOEC, Anaheim, CA, March 2013, paper OW3G.1

[4] Tucker, R.S.: Green optical communications—part I: energy limitations in transport. J. Sel. Quantum Electron. **17**(2), 245–260 (2011)

[5] Cvijetic, N., Qian, D., Hu, J.: 100 Gb/s optical access based on optical orthogonal frequency-division multiplexing. IEEE Commun. Mag. **48**(7), 70–77 (2010)

[6] Effenberger, F.J.: The XG-PON system: cost effective 10 Gb/s access. J. Lightwave Technol. **29**(4), 403–409 (2011)

[7] Fouli, K., Maier, M.: Ocdma and optical coding: principles, applications, and challenges. IEEE Commun. Mag. **45**(8), 27–34 (2007)

[8] Yin, H., Richardson, D.J.: Optical Code Division Multiple Access Communication Networks: Theory and Applications. Springer, Berlin (2009)

[9] Kamath, P., Touch, J.D., Bannister, J.A.: The need for media access control in optical CDMA networks. In: Proceedings of IEEE Conference Computer Communications (Infocom '04), pp. 2208–2219, March 2004

[10] Raad, R., Inaty, E., Fortier, P., Shalaby, H.M.H.: Optimal resource allocation scheme in a multirate overlapped optical CDMA system. J. Lightwave Technol. **25**(8), 2044–2053 (2007)

[11] Inaty, E., Raad, R., Fortier, P., Shalaby, H.M.H.: A fair QoS-based resource allocation scheme for a time-slotted optical OV-CDMA packet networks: a unified approach. J. Lightwave Technol. **26**(21), 1–10 (2009)

[12] Khaleghi, S., Pakravan, M.R.: Quality of service provisioning in optical CDMA packet networks. J. Opt. Commun. Netw. **2**(5), 283–292 (2010)

[13] Inaty, E., Raad, R., Fortier, P., Shalaby, H.M.H.: Performance comparison between S-ALOHA and $R^3T$ protocols for multirate OFFH-CDMA systems in optical packet networks. J. Opt. Netw. **5**(12), 927–936 (2006)

[14] Durand, F.R., Filho, M.S., Abrão, T.: The effects of power control on the optical CDMA random access protocol. Opt. Switch. Netw. **9**(1), 52–60 (2012)

[15] Tang, M., Long, C., Guan, X.: Nonconvex optimization for power control in wireless CDMA networks. Wirel. Pers. Commun. **58**(4), 851–865 (2011)

[16] Durand, F., Abrão, T.: Energy-efficient power allocation for WDM/OCDM networks with particle swarm optimization. J. Opt. Commun. Netw. **5**(5), 512–523 (2013)

[17] Kwong, W.C., Yang, G.-C.: Multiple-length extended carrier-hopping prime codes for optical CDMA systems supporting multirate multimedia services. J. Lightwave Technol. **23**(12), 3653–3662 (2009)

[18] Shalaby, H.M.H.: Optical CDMA random access protocols with and without pretransmission coordination. J. Lightwave Technol. **21**, 2455–2462 (2003)

[19] Shalaby, H.M.H.: Performance analysis of an optical CDMA random access protocol. J. Lightwave Technol. **22**(5), 1233–1241 (2004)

[20] Mohamed, M.A.A., Shalaby, H.M.H., El-Badawy, E.A.: Performance analysis of an optical CDMA MAC protocol with variable-size sliding window. J. Lightwave Technol. **24**(10), 3590–3597 (2006)

[21] Mohamed, M.A.A., Shalaby, H.M.H., El-Badawy, E.A.: Optical code-division multiple-access protocol with selective retransmission. SPIE Opt. Eng. **45**(5), 055007(1–8) (2006)

[22] El-Sahn, Z.A., Abd-El-Malek, Y.M., Shalaby, H.M.H., El-Badawy, E.A.: Performance of the $R^3T$ random-access OCDMA protocol in noisy environment. IEEE J. Sel. Top. Quantum Electron. **13**, 1396–1402 (2007)

[23] Raad, R., Inaty, E., Fortier, P., Shalaby, H.M.H.: Optical S-ALOHA/CDMA systems for multirate applications: architecture, performance evaluation, and system stability. J. Lightwave Technol. **24**, 1968–1977 (2006)

[24] Sun, S., Yin, H., Wang, Z., Xu, A.: Performance analysis of a new random access protocol for OCDMA networks. Photon Netw. Commun. **14**(1), 89–995 (2007)

[25] Shoaie, M.A.: Performance analysis of slotted ALOHA random access packet-switching optical CDMA networks using generalized optical orthogonal codes and M-ary overlapping PPM signaling. J. Opt. Netw. **3**(7), 568–576 (2011)

[26] Brès, C.-S., Prucnal, P.R.: Code-empowered lightwave networks. J. Lightwave Technol. **25**(10), 2911–2921 (2007)

[27] Shannon, C.E.: The mathematical theory of communication. Bell Syst. Tech. J. **27**, 379–423 (1948). (reprinted with corrections 1998)

[28] Tarhuni, N., Korhonen, T., Elmusrati, M., Mutafungwa, E.: Power control of optical CDMA star networks. Opt. Commun. **259**, 655–664 (2006)

[29] Forney, G.D., Ungerboeck, G.: Modulation and coding for linear Gaussian channels. IEEE Trans. Inf. Theory **44**(6), 2384–2415 (1998)

[30] Sampaio, L., Abrão, T., Angelico, B., Lima, M., Proença, M., Jeszensky, P.: Hybrid haceuristic-waterfilling game theory approach in MC-CDMA resource allocation. Appl. Soft Comput. **12**, 1902–1912 (2011)

[31] Golub, G.H., Van Loan, C.F.: Matrix Computations, 3rd edn. Johns Hopkins University Press, Baltimore (1996)

[32] Durand, F., Angelico, T., Abrão, T.: Delay and estimation uncertainty in distributed power control algorithm for optical CDMA networks. Opt. Switch. Netw. **21**, 67–78 (2016)

[33] Aurzada, F., Scheutzow, M., Reisslein, M., Ghazisaidi, N., Maier, M.: Capacity and delay analysis of next-generation passive optical networks (NG-PONs). IEEE Trans. Commun. **59**(5), 1378–1388 (2011)

[34] Miyata, S., Baba, K., Yamaoka, K., Kinoshita, H.: Exact mean packet delay analysis for long-reach passive optical networks. In: 2015 IEEE Global Communications Conference (GLOBECOM), pp. 1–6

[35] Rad, M.M., Fathallah, H., Rusch, L.A.: Fiber fault PON monitoring using optical coding: effects of customer geographic distribution. IEEE Trans. Commun. **58**(4), 1172–1181 (2010)


**Fábio Renan Durand** received the M.S. degree in electrical engineering from the São Carlos Engineering School of São Paulo State, Brazil, in 2002 and Ph.D. degree in electrical engineering from the State University of Campinas (UNICAMP), São Paulo, Brazil, in 2007. Now he is a Professor at Technologic Federal University of Paraná (UTFPR) at Cornélio Procópio, Brazil. His research interest has been photonic technology, WDM/OCDM and Elastic Optical Networks, heuristic and optimization aspects of optical networks and physical impairments.

**Taufik Abrão** (SM'12) received the B.S., M.Sc., and Ph.D. degrees in electrical engineering from the Polytechnic School of the University of São Paulo, São Paulo, Brazil, in 1992, 1996, and 2001, respectively. Since March 1997, he has been with the Communications Group, Department of Electrical Engineering, Londrina State University, Londrina, Brazil, where he is currently an Associate Professor of Communications engineering. In 2012, he was an Academic Visitor with the Communications, Signal Processing and Control Research Group, University of Southampton, Southampton, U.K. From 2007 to 2008, he was a Postdoctoral Researcher with the Department of Signal Theory and Communications, Polytechnic University of Catalonia (TSC/UPC), Barcelona, Spain. He has participated in several projects funded by government agencies and industrial companies. He is involved in editorial board activities of six journals in the communication area and he has served as TCP member in several symposium and conferences. He has been served as an Editor for the IEEE COMMUNICATIONS SURVEY & TUTORIALS since 2013. He is a member of SBrT and a senior member of IEEE. His current research interests include communications and signal processing, specially the multi-user detection and estimation, MC-CDMA and MIMO systems, cooperative communication and relaying, resource allocation, as well as heuristic and convex optimization aspects of 3G and 4G wireless systems. He has co-authored of more than 170 research papers published in specialized/international journals and conferences